ELSEVIER

Solid State Ionics 140 (2001) 263–274

SOLID STATE IONICS

www.elsevier.com/locate/ssi

Rare earth cuprates as electrocatalysts for methanol oxidation

V. Raghuveer [a], K. Ravindranathan Thampi [b], N. Xanthopoulos [c], H.J. Mathieu [c], B. Viswanathan [a,*]

[a] *Department of Chemistry, Indian Institute of Technology, Madras, Chennai 600 036, India*
[b] *Laboratory of Photonics and Interfaces, Ecole Polytechnique Federale de Lausanne, Lausanne CH-1015, Switzerland*
[c] *Surface Analysis Laboratory, Department of Materials, Ecole Polytechnique Federale de Lausanne, Lausanne CH-1015, Switzerland*

Received 30 June 2000; received in revised form 13 February 2001; accepted 19 February 2001

Abstract

A series of rare earth cuprates with overall composition $Ln_{2-x}M_xCu_{1-y}M'_yO_{4-\delta}$ (where Ln = La and Nd; M = Sr, Ca and Ba; M′ = Ru and Sb: $0.0 \leq x \leq 0.4$ and $y = 0.1$) have been tested as anode electrocatalysts for methanol oxidation. The evaluation of electrode kinetic parameters was made galvanostatically. The catalyst characterization was carried out by specific conductivity measurements, X-ray diffraction (XRD), X-ray photoelectron spectroscopy (XPS) and Iodometry. These materials exhibit significant activity for methanol oxidation at higher potentials. The linear correlation between $Cu(3+)$ content and methanol oxidation activity suggests that the active sites for adsorption of methanol is $Cu(3+)$. The methanol oxidation onset potential depends on the ease of $Cu(2+) \rightarrow Cu(3+)$ oxidation reaction. These materials show better tolerance towards the poisoning by the intermediates of methanol oxidation compared to that of conventional noble metal electrocatalysts (supported and bulk). The lattice oxygen in these oxides could be considered as active oxygen to remove CO intermediates of methanol oxidation reaction.

Keywords: Rare earth cuprates; Electrocatalyst; Fuel cell electrodes; Perovskite; Methanol oxidation

1. Introduction

The search for less expensive alternative materials as anodes for direct methanol fuel cells (DMFC) has been a topic of current interest. Conventionally, noble metals such as Pt, Pt–Ru bimetallic systems have been employed as electrocatalysts for methanol oxidation in acid and alkaline media [1,2]. Noble metal sites are known to be poisoned by the methanol oxidation intermediates like CO species formed during the oxidation reaction. This accounts for the experimentally observed deterioration in the performance of noble metal-based fuel cell electrodes. Several ambient temperature direct methanol fuel cells have been reported employing dispersed platinum-based electrocatalysts in polymer electrolyte (Nafion 117). The applicability of Pt-based electrodes is restricted because of the accumulation of surface poisoning intermediates, thus leading to loss in activity with time. One way of avoiding the poisoning phenomenon is to alloy the platinum with the oxophylic metal such as Ru and Sn. Another approach to avoid such poisoning phenomenon is to employ electronically conducting mixed oxides as

* Corresponding author. Tel.: +91-44-4458250; fax: +91-44-2355029.
E-mail address: bviswanathan@hotmail.com (B. Viswanathan).

0167-2738/01/$ - see front matter
PII: S0167-2738(01)00816-5

anode materials. Though various attempts have been made earlier to use oxides of V, Fe, Ni, In, Sn, La and Pb as anode materials [3], none of them have shown any measurable activity for methanol oxidation except NiO. In recent years, studies on various transition metal mixed oxides have shown the applicability of perovskite oxides as substitutes for noble metals as fuel cell electrodes at high temperatures [4–9]. Oxidation of methanol involves oxidative dehydrogenation as the first step. This is related to the surface basicity of the oxide. Thus, the desirability for having alkaline earth or lanthanide ions at the electrocatalyst surface can be seen. This has led us to examine lanthanum-based oxides as substitutes for noble metal-based electrodes. In the present investigation, a study was carried out using a series of rare earth cuprates of composition $Ln_{2-x}M_xCu_{1-y}M'_yO_{4-\delta}$ (where Ln = La and Nd; M = Sr, Ca and Ba; M′ = Ru and Sb; $0.0 \leq x \leq 0.4$ and $y = 0.1$) as anode materials in alkaline medium. Alkaline medium was chosen since these materials are unstable in acid medium. These materials possess high electronic conductivity at room temperature [10,11], sufficient oxide ion diffusivity [12–14] and displayed appreciable gas phase heterogeneous catalytic activity for the dehydrogenation of methanol and oxidation of CO at temperatures around 200°C [15]. As it is known that methanol electro-oxidation involves dehydrogenation as a first step followed by oxidation of CO to CO_2, it was considered worthwhile to examine the electrocatalytic properties of these systems.

2. Experimental

2.1. Electrocatalysts preparation

The rare earth cuprates of composition $Ln_{2-x}M_xCu_{1-y}M'_yO_{4-\delta}$ (where Ln = La and Nd; M = Sr, Ca and Ba; M′ = Ru and Sb; $0.0 \leq x \leq 0.4$ and $y = 0.1$) were prepared by conventional solid state method. Appropriate amounts of rare earth oxide (CDH, 99.99%), alkaline earth metal carbonates (S.d. fine Chemicals) and corresponding transition metal oxide were well mixed followed by firing at 950°C for 24 h with intermediate grinding at 12 h. The catalysts thus obtained were characterized by X-ray diffraction (XRD) using Rigaku miniflex instrument with Fe-filtered CoK_α radiation.

2.2. Electrode fabrication

Disk type electrodes of 12 mm diameter were fabricated as described in our previous communication [16], pelletizing 0.3 g of oxide by applying a pressure of 5 tonnes. The electrical contact was made by attaching copper leads onto the back face of the pellet with silver paint. The sample was then mounted onto a glass holder, and epoxy resin was used to insulate the electrode from the electrolyte solution on all but faces except the front of the pellet.

Carbon-based electrodes were also prepared by a roll bonded technique, in which the catalyst was well mixed with carbon in 3:1 ratio followed by the addition of 1:1 mixture of water and THF. The PTFE emulsion was added as a binder in 3:4 (Cat:PTFE) ratio followed by ultrasonification for 45 min. The resulting semi-solid paste thus obtained was spread onto the previously teflonised carbon cloth and levelled using a roller.

2.3. Electrochemical measurements

Electrochemical measurements were carried out with the electrode mounted in a conventional three electrode cell having a porous glass separator between the working and counter electrode. The Platinum foil (1 cm^2 area) and Hg/HgO were used as counter and reference electrodes, respectively. The electrochemical oxidation of methanol was carried out in 3 M KOH and 1 M methanol at room temperature. The cyclic voltammograms were recorded with Potentioscan Wenking Model POS 73 and Philips X-Y recorder. All the oxide samples were given electrochemical pretreatment by potential cycling between -0.24 and $+0.9$ V in alkali for 30 min in order to get reproducible voltammograms. For both disk type and carbon-based electrodes, there was no significant change in the characteristics of the voltammogram.

The Tafel plots were constructed in the galvanostatic mode. The equilibration time given before the starting of the experiment in the presence of methanol is 18 h.

Roughness factor for the Sr-substituted oxides was determined using cyclic voltammetry [8]. The charging current in the double layer region was

measured at different scan rates. From the slope of the charging current vs. scan rate, the value of C_{dl} was obtained and the roughness factor was determined using the formula $R = C_{dl}/C^*$ (where C^* is Theoretical roughness factor for oxides, the value is 60 $\mu F/cm^2$).

The electrode stability of these oxidic electrode materials was tested by constructing current vs. time plots.

2.4. Specific conductivity and PZC measurements

Room temperature specific conductivity for the oxides was measured using DC-four probe method. Sintered pellets (12 mm in diameter and ca. 2 mm thick) were prepared by pressing powdered material at 5 tonnes followed by firing at 950°C for 24 h.

The pH of zero charge (PZC) of oxide particles prepared by solid state reaction was determined by potentiometric acid–base titration [17]. A weighed quantity of oxide powder was suspended in 0.005 M KNO_3 solution for 1 h during which N_2 gas was bubbled through the solution to prevent any contamination from the CO_2 present in the atmosphere. The pH of the solution was brought to the basic side by the addition of known amount of 0.1 M KOH. The suspension was titrated with 0.1 M HNO_3. After the pH became stable, the readings were recorded at each point. The intersection point of the titration curve obtained in the presence of oxide and that of the previously obtained for the blank solution gives the PZC of the oxide particles.

2.5. Determination of Cu^{3+} content and oxygen nonstoichiometry

The Cu^{3+} content of various Sr containing lanthanum cuprates was determined by an Iodometric titration technique [18]. The value of δ (oxygen nonstoichiometry) was obtained using the mean valence of copper ions with the charge neutrality condition.

2.6. Surface characterization by X-ray photoelectron spectroscopy

The surface characterization was carried out by X-ray photoelectron spectroscopy with Axis Ultr Kratos instrument using Al K_α as X-ray source.

2.7. Structural stability characterization by XRD

Structural stability of the oxides was verified by recording XRD before and after methanol oxidation for 30 min at a fixed potential of +0.7 V vs. Hg/HgO.

3. Results and discussion

3.1. Cyclic voltammogram characterization of strontium-substituted rare earth cuprate

Typical cyclic voltammogram obtained for the strontium-substituted rare earth cuprate of composition $La_{1.9}Sr_{0.1}CuO_4$ as electrode in 3 M KOH is shown in Fig. 1a. The cathodic peak between +0.06 and −0.24 V is attributed to the reduction (surface $Cu(3+/2+)$) of the electrode [19]. The anodic peak between +0.26 and +0.5 V can be due to the oxidation of the electrode, since this is much more cathodic than the oxygen evolution potential. Moreover, the charge due to the anodic peak corresponds to the one electron transfer reaction.

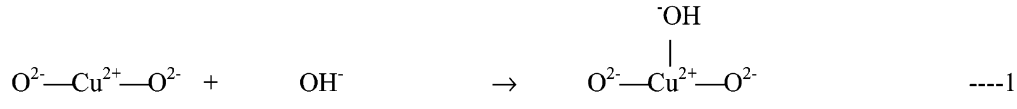

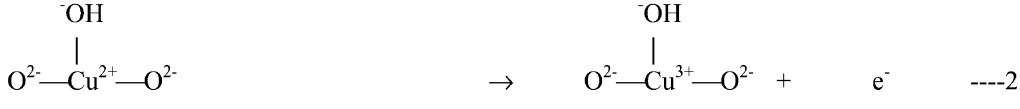

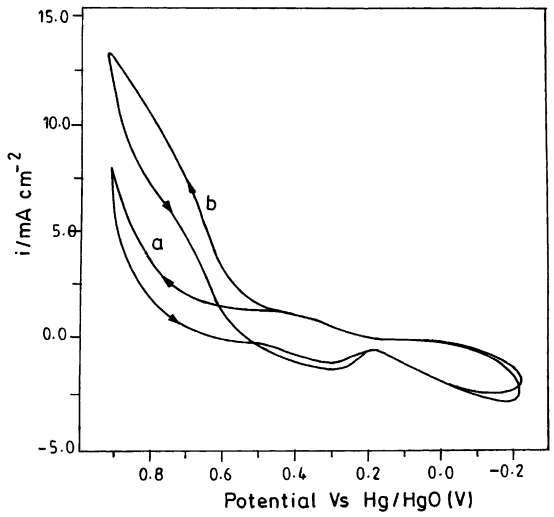

Fig. 1. Cyclic voltammogram of $La_{1.9}Sr_{0.1}CuO_4$ (a) in 3 M KOH and (b) 3 M KOH and 1 M CH_3OH mixture at 300 K at a scan rate of 25 mV s^{-1}.

The anodic current obtained at potentials greater than +0.7 V is due to the oxygen evolution reaction. A cathodic peak between +0.46 and +0.26 V was observed after sweeping the potential for 30 min. In order to assign this cathodic peak, the following experiment was performed. The electrode was polarized at +0.7 V for 30 min, then the cyclic voltammogram was recorded in which the cathodic peak was observed. After the solution was purged with N_2 gas at the open circuit potential for 30 min, the cathodic peak current between +0.46 and +0.26 V, which was observed earlier, decreased almost to the minimum. Therefore, it is deduced that this cathodic peak can be due to the reduction of the high-pressure oxygen trapped inside the pores as suggested by Yeung and Tseung [20].

The cyclic voltammogram obtained for the electro-oxidation of methanol using the oxide of composition $La_{1.9}Sr_{0.1}CuO_{4-\delta}$ as anode is shown in Fig. 1b. It is seen that the methanol oxidation onset potential is at +0.46 V, whereas all other peaks in the voltammogram are similar to the cyclic voltammograms obtained without methanol. From Fig. 1b, it is seen that Cu(2+/3+) redox reaction precedes the methanol oxidation in the anodic sweep suggesting that the methanol oxidation starts after the oxidation of Cu(2+) to Cu(3+). Similar observation was made by the Fleischmann et al. [21] for the NiO electrodes as anodes for methanol oxidation. They proposed the catalytic role of Ni(3+) which was also supported by results reported by El-Shafei [22,23].

In alkaline medium, the carbon dioxide formed will form carbonates. The amount of carbonates formed during methanol oxidation in the electrolyte was quantitatively estimated using the method reported in literature [24] and was found to be 0.038 M.

The charge in the potential region between +0.1 and +0.4 V was measured from the cyclic voltammogram in the presence and absence of methanol. This was found to be 5.41 mC ($Q_{Cu(2+)\rightarrow Cu(3+)}$ and $Q_{ads(methanol)}$) and 1.01 mC ($Q_{Cu(2+)\rightarrow Cu(3+)}$), respectively. The difference between these charge values (4.40 mC) gives the charge due to the adsorption of methanol. Thus, the potential region between +0.1 and +0.4 V was assumed to be the methanol adsorption region in this investigation.

3.2. Effect of Sr content in the A lattice site

The properties of the perovskite type oxides are generally quite sensitive to the nature of A-site ions [12,25]. On substitution of Sr ions at the A-site, the charge neutrality is maintained by the formation of oxygen vacancies and as well as by the change in the valence state of the copper ions. This increases both the electronic conductivity and oxide ion conductivity due to the mixed valence of copper ions and oxygen vacancy.

In order to evaluate the role of Cu(3+) ions in methanol oxidation, the concentration of Cu(3+) was varied by altering the content of Sr at the A sub-lattice. The electrocatalytic activity of Sr-substituted lanthanum cuprates of compositions $La_{2-x}Sr_xCuO_{4-\delta}$ (where $0.0 \le x \le 0.4$) for methanol oxidation was evaluated by measuring the current at +0.7 V. The results obtained are shown in Table 1. It is seen from Table 1 that the methanol oxidation activity increases with increase in Sr content at the A-site till $x = 0.2$, then drops with further increase in Sr content. This change in activity was found to have good correlation with the Cu(3+) content, which was determined iodometrically (refer to Table 1). The maximum activity corresponds to the compo-

Table 1
Physico-chemical properties of Sr-substituted lanthanum cuprates

Electrocatalysts	Specific conductivity (Ω^{-1} cm^{-1})	Cu(2+)	Cu(3+)	Oxygen nonstoichiometry (δ)	C_{dl} (F/cm^2)	I^a (mA cm^{-2})	R_f
La_2CuO_4	0.28	1.0	0.0	0.0	–	5.0	–
$La_{1.9}Sr_{0.1}CuO_4$	18.27	0.921	0.079	0.011	1×10^{-2}	8.0	167
$La_{1.8}Sr_{0.2}CuO_4$	67.56	0.856	0.144	0.028	–	14.0	–
$La_{1.7}Sr_{0.3}CuO_4$	16.97	0.938	0.062	0.098	6.5×10^{-3}	0.68	108
$La_{1.6}Sr_{0.4}CuO_4$	10.30	0.975	0.026	0.186	7.5×10^{-4}	0.50	12.5

C_{dl}—Double layer capacitance; R_f—roughness factor.
[a]At +0.7 V vs. Hg/HgO.

sition having $x = 0.2$ where it has the maximum Cu(3+) concentration. This suggests that Cu(3+) could be the active sites for methanol oxidation.

The electrocatalytic activity depends on both electronic and geometric factors [2,8,17]. The former is governed by the electronic structure and the nature of the active sites, whereas the latter is determined by the surface concentration of the active sites and the extent of actual surface area. Separation of electronic from geometric factor is essential for proper understanding of the origin of electrocatalytic activity as well as to optimize electrode selection. Separation is probably possible by two means: (i) measurement of actual surface area and (ii) evaluation of surface acid–base properties of oxides in aqueous solution. The latter is an intensive property that does not depend on the surface area of the oxides but only on the nature of the active sites. The actual surface area measurements are difficult in the case certain electrode materials. The surface acid–base properties can be measured for the oxides by determining the pH of zero charge (PZC), i.e. the pH at which the oxide surface is electrically and chemically neutral. The PZC is a measure of Lewis acidity [8]. The plot of PZC vs. Sr content is shown in Fig. 2. The intriguing point is that the variation of the PZC appears to parallel with that of the electrocatalytic properties. So the PZC can be used as a parameter to separate electronic and geometric factors.

3.3. Electrode tolerance for oxidation intermediates

Our main aim is to compare the electrode tolerance for the oxidation intermediates irrespective of the applied potential and reaction rates. The electrode stability of these systems was compared with that of supported and unsupported platinum for methanol oxidation. The plot of current vs. time was made by applying a constant methanol oxidation potential of +0.7 and −0.1 V for the Sr-substituted compositions and platinum, respectively. In these plots, there is an initial decay in the current, and then it becomes stable. From the slopes of the current decaying region, the rates of deactivation were calculated and the values are given in Table 2.

It is seen from Table 2 that the rate of deactivation is significantly higher for supported and bulk platinum compared to that of the strontium-substituted lanthanum cuprates during methanol oxidation. The high rate of deactivation value for platinum during methanol oxidation can be well understood due to the accumulation of poisoning intermediates

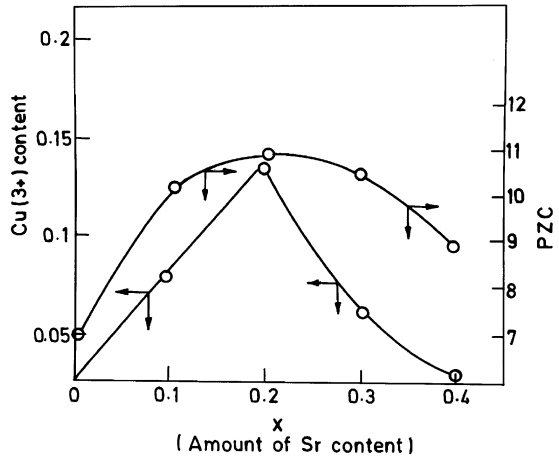

Fig. 2. Variation of Cu(3+) content and PZC as a function of strontium content in $La_{2-x}Sr_xCuO_4$ ($0.0 \le x \le 0.4$).

Table 2
Rate of deactivation values for Sr-substituted lanthanum cuprates and platinum anode electrocatalysts

Electrocatalysts	Rate of deactivation (mA/min)
La_2CuO_4	0.42
$La_{1.9}Sr_{0.1}CuO_4$	0.36
$La_{1.7}Sr_{0.3}CuO_4$	0.03
$La_{1.6}Sr_{0.4}CuO_4$	0.05
Bulk Pt	16.56
Supported Pt (Pt/C)	5.2

such as CO on the surface of the electrode. This accumulation takes place on Pt surfaces because of the lack of active oxygen on the surface. In order to overcome this, Pt–Ru bimetallic catalyst is employed [2], in which Ru provides active oxygen to remove methanol oxidation intermediate such as CO on the platinum surface as CO_2 effectively.

The lower value of rate of deactivation for the Sr-substituted oxides may suggest that these electrodes are capable of removing the strongly bound oxidation intermediates of methanol formed on the oxide surface. These materials possess better tolerance towards the oxidation intermediates compared to that of the platinum. It is not clear at present the nature of the oxidation intermediate formed on the oxide surface.

To remove oxidation intermediates CO as CO_2, an active oxygen is required. In order to see whether the active oxygen comes from the solution or from the substituted oxide itself, the methanol oxidation was performed by continuously purging the electrolyte with (i) O_2 gas to saturate the solution and (ii) N_2 gas to remove the dissolved oxygen. The electrocatalytic activity was not affected either in the presence or absence of oxygen suggesting the involvement of lattice oxygen in the oxidation reaction.

3.4. Influence of oxygen nonstoichiometry on the electrode tolerance for the oxidation intermediates

It was observed that the rate of deactivation decreases with increase in the strontium content at the A sub-lattice. The rate of deactivation has a correlation with the increase in the oxygen nonstoichiometry, which is shown in Fig. 3. This correlation suggests the involvement of lattice oxygen in oxidizing methanol. The lattice oxygen may combine with the oxidation intermediates as and when they are formed on the oxide surface. The ease with which the lattice oxygen combines with the oxidation intermediates is an important step in accounting for the electrode tolerance for the oxidation intermediates. The replacement of $La(3+)$ by $Sr(2+)$ results in increase in concentration of oxygen vacancy and also results in increase of O^{2-} diffusivity [26]. Based on Nakamura et al. [27], the desorption of lattice oxygen is easier with increase in $Sr(2+)$ content because of the increased tolerance for oxygen vacancies. The O^{2-} ion transport to the reaction site may be enhanced, which may be responsible for the decrease in the rate of deactivation on increasing the Sr content at the A-site for the oxidation of methanol.

3.5. X-ray photoelectron spectroscopy

The X-ray photoelectron spectra of the oxide of composition $La_{1.8}Sr_{0.2}CuO_4$ were recorded for the Cu 2p region before and after methanol oxidation for 14 h. The spectra are shown in Fig. 4. In Fig. 4a, the two peaks with binding energies 933.2 and 952.8 eV correspond to emissions from $Cu_{2p3/2}$ and $Cu_{2p1/2}$ levels, respectively. These binding energy values

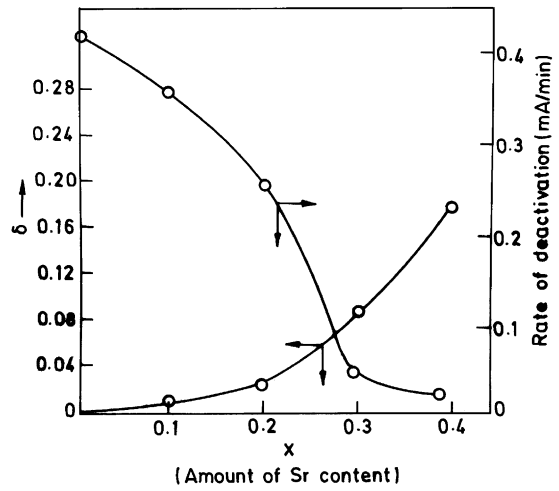

Fig. 3. Variation of oxygen nonstoichiometry (δ) and rate of deactivation as a function of strontium content in $La_{2-x}Sr_xCuO_4$ ($0.0 \le x \le 0.4$).

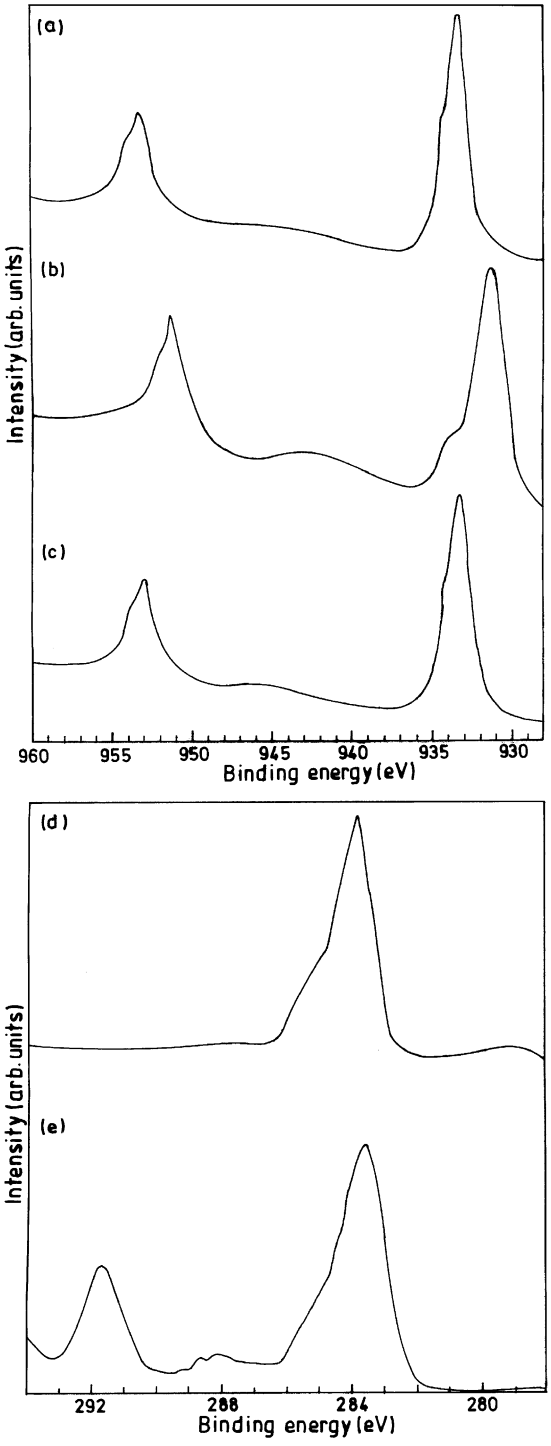

indicate that Cu is present in +2 oxidation state in the starting material. There are two shoulders observed at 934.4 and 953.9 eV. This may indicate the presence of other oxidation states. However, there is no definite assigned binding energies for Cu in the +3 oxidation state. In Fig. 4b, the XP spectrum of the oxide after methanol oxidation is given. The $Cu_{2p3/2}$ and $Cu_{2p1/2}$ emissions are shifted to lower binding energy which are centered at 931.5 and 951.5 eV with FWHM being higher, suggesting that some of the Cu is reduced to lower oxidation state. The XP spectrum recorded taken for the oxide after methanol oxidation and after etching is shown in Fig. 4c, the original $Cu_{2p3/2}$ and $Cu_{2p1/2}$ peak positions are restored as in Fig. 4a suggesting the change in the oxidation state of Cu took place only on the surface not in the bulk. The XP spectrum was recorded in the carbon 1s region before and after methanol oxidation is shown in Fig. 4d and e. The signal at 292 eV might be attributed to Sr carbonate species or adsorbed residues of methanol.

The XRD pattern of the oxide before and after methanol oxidation are the same suggesting that no structural transformation of oxide phase has taken place during the oxidation reaction.

The analysis of the electrolyte for dissolved copper from $La_{2-x}Sr_xCuO_{4-\delta}$ by ICPES showed that compositions containing lower strontium content exhibited copper dissolution, while systems with higher Sr content (≥ 0.2), the dissolution is significantly lower (< 0.02 ppm).

3.6. Effect of the nature of rare earth in the A-site

The methanol oxidation was carried out for the electrodes of composition $Ln_{1.8}Sr_{0.2}CuO_4$ (Ln = La and Nd), which showed that the onset potential was lower for Nd containing compound (refer data in Table 3). The Sm and Dy containing compositions were prepared but the single phase compound could not be obtained.

Fig. 4. X-ray photoelectron spectra of $La_{1.8}Sr_{0.2}CuO_{4-\delta}$ taken in the $Cu_{2p3/2}$ and $Cu_{2p1/2}$ region (a) before methanol oxidation, (b) after methanol oxidation before etching, (c) after methanol oxidation after etching, (d) C_{1s} region before oxidation, and (e) C_{1s} region after methanol oxidation.

Table 3
Methanol oxidation onset potentials for substituted rare earth cuprates

Electrocatalysts	Methanol oxidation onset potential (V vs. Hg/HgO)
$La_{1.9}Sr_{0.1}CuO_4$	0.46
$La_{1.9}Ca_{0.1}CuO_4$	0.51
$La_{1.9}Ba_{0.1}CuO_4$	0.78
$Nd_{1.8}Sr_{0.2}CuO_4$	0.35
$La_{1.9}Sr_{0.1}Cu_{0.9}Sb_{0.1}O_4$	0.34
$La_{1.9}Sr_{0.1}Cu_{0.9}Ru_{0.1}O_4$	0.76

3.7. Effect of the nature of alkaline earth metal cation at the A sub-lattice

The methanol oxidation was performed for the electrodes of composition $La_{1.8}M_{0.2}CuO_4$ (where M = Sr, Ca and Ba) by varying the nature of alkaline earth metal at the A-lattice site. The methanol oxidation onset potential was found to follow the order Sr < Ca < Ba (refer data in Table 3).

3.8. Effect of the partial substitution at the B-site

The methanol oxidation was carried out for the electrode of composition $La_{1.9}Sr_{0.1}Cu_{0.9}M'_{0.1}O_4$ (M′ = Ru and Sb) in alkaline medium. This forms a series of solid solution in the range $0 \le y \le 1$ [28]. The methanol oxidation onset potential was found to follow the order:

$$La_{1.9}Sr_{0.1}Cu_{0.9}Ru_{0.1}O_4\,(0.76\,V) > La_{1.9}Sr_{0.1}CuO_4\,(0.46\,V) > La_{1.9}Sr_{0.1}Cu_{0.9}Sb_{0.1}O_4\,(0.34\,V).$$

The values in the brackets represent the methanol oxidation onset potentials.

The cyclic voltammogram of the partially substituted B-site compositions in the potential region of Cu(2 + /3 +) redox reaction is shown in Fig. 5. The vertical dotted line shown in the figure represents the mean potential of the oxidation of Cu(2 +) to Cu(3 +) reaction. It is seen from the figure that the shift in the redox potential caused by the partial substitution at the B-site appears to be reflected in the methanol oxidation onset potential also. The direction of the shift of redox potential reflects qualitatively the thermodynamic feasibility of the oxidation of Cu(2 +) to Cu(3 +) [29]. By extending the Goodenough model proposed for ruthenates, the separation between the energies of the oxidized and the reduced forms varies when the substitution is effected at the B-site.

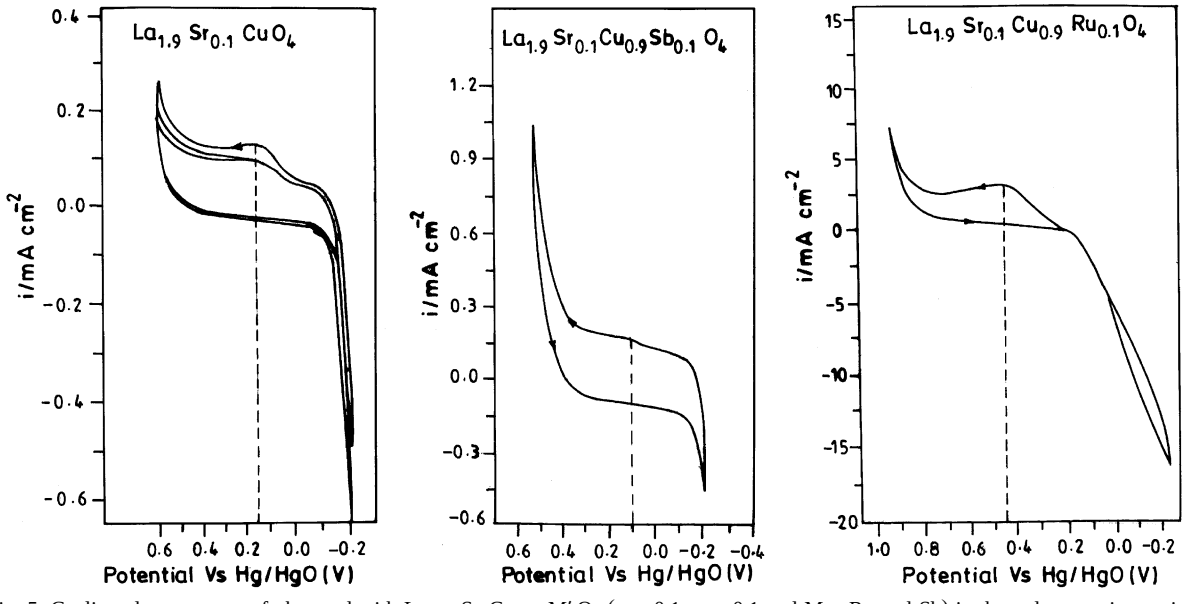

Fig. 5. Cyclic voltammogram of observed with $La_{2-x}Sr_xCu_{1-y}M'_yO_4$ ($x = 0.1$; $y = 0.1$ and M = Ru and Sb) in the redox reaction region in 3 M KOH at 300 K at a scan rate of 25 mV s^{-1}.

It was mentioned earlier that the Cu(3 +) could be the active site for methanol oxidation in the substituted cuprates. So the potential at which the Cu(3 +) forms naturally reflects on the onset potential for methanol oxidation. In the case of Sb-substituted compositions, the redox potential shifts cathodically by 0.06 V with respect to the unsubstituted composition. Therefore, substitution of Cu with small amount of Sb(5 +) at the B-site will permit easier oxidation of Cu(2 +) to Cu(3 +). Hence, methanol oxidation onset potential shifts cathodically for Sb-substituted composition by 0.12 V with respect to the unsubstituted composition. In the case of Ru-substituted composition, the presence of small amount of Ru(+ 5) [28] in the B-site shifts the redox potential anodically by 0.26 V with respect to the unsubstituted composition. The oxidation of Cu(2 +) to Cu(3 +) is no longer easier and takes place only at higher potential, hence methanol oxidation onset potential moves anodically by 0.3 V with respect to the unsubstituted composition. Thus, the methanol oxidation onset potential depends on the thermodynamic feasibility of Cu(2 +) → Cu(3 +), which can be altered when the Cu(2 +) ions are substituted with suitable valent transition metal ions.

3.9. Mechanism of electro-oxidation of methanol on oxide surface

The mechanism of methanol oxidation on perovskite electrocatalytic sites can be speculated as follows: Methanol is initially adsorbed on the perovskite transition metal ion sites on the B-lattice, while simultaneously losing its alcoholic proton to a basic oxide ion. The methoxy species formed get oxidatively decomposed to CO species. This strongly bound intermediate is then expected to be removed from the electrocatalyst surface by the reaction with surface lattice oxide species. The resulting oxygen ion vacancy in the perovskite will then be replenished by reacting with water or OH^- from the electrolyte.

3.9.1. Speculative mechanism of methanol oxidation on the oxide surface

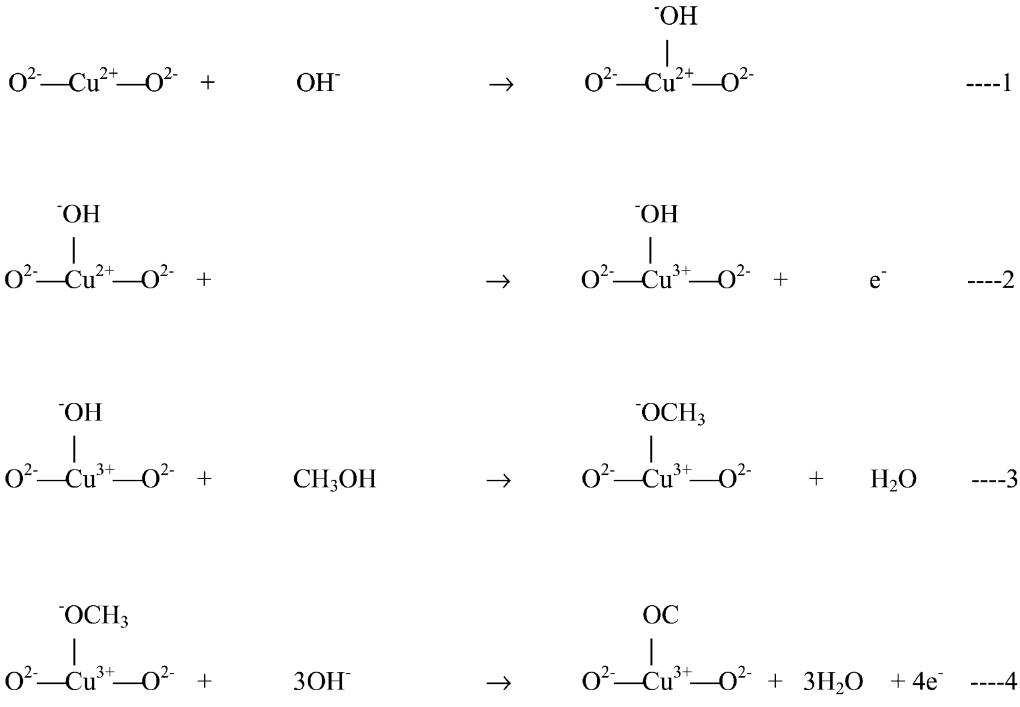

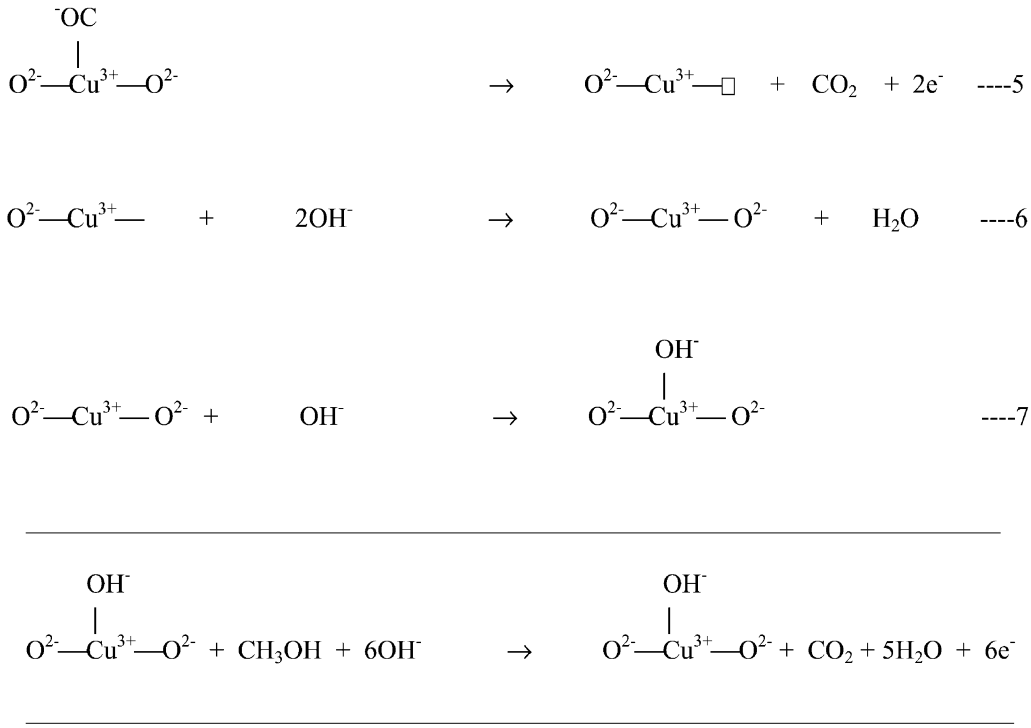

The Tafel plots constructed for these substituted rare earth cuprates in galvanostatic mode are shown in Fig. 6. The values of Tafel slope measured for the Sb-substituted and unsubstituted lanthanum cuprates in the methanol adsorption region are given in Table 4. From the values given in Table 4, it is seen that the value of Tafel slope in the methanol adsorption region for the rare earth cuprates is almost twice that

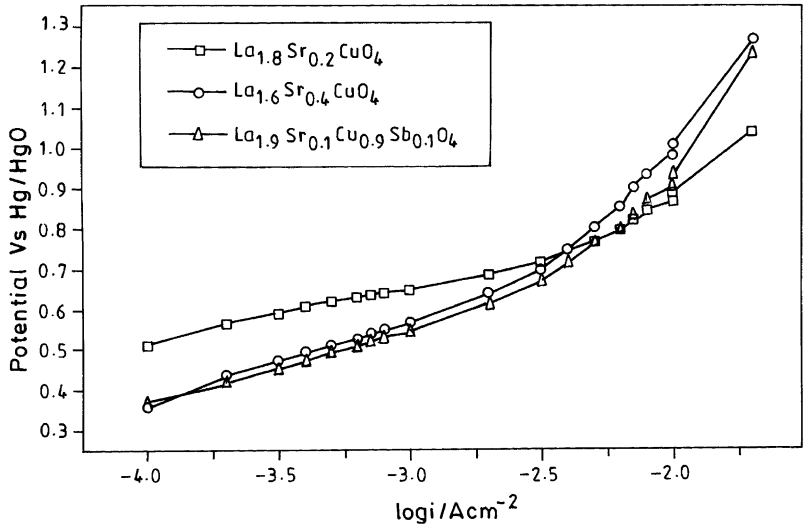

Fig. 6. Tafel plots for substituted rare earth cuprates at 300 K in 3 M KOH and 2 M CH_3OH mixture.

Table 4
Tafel slope in the methanol adsorption region for Sr-substituted lanthanum cuprates and platinum

Catalyst	Tafel slope (V/decade)
Pt	0.098
$La_{1.8}Sr_{0.2}CuO_4$	0.180
$La_{1.9}Sr_{0.1}Cu_{0.9}Sb_{0.1}O_4$	0.155

Table 5
Values of apparent exchange current density for Sr-substituted lanthanum cuprates and platinum

Electrocatalysts	Apparent exchange current density (A/cm^2)
Pt	$\sim 10^{-3}$
$La_{1.8}Sr_{0.2}CuO_4$	1.78×10^{-4}
$La_{1.9}Sr_{0.1}Cu_{0.9}Sb_{0.1}O_4$	6.3×10^{-4}

obtained for the platinum. However, there is a slight decrease in Tafel slope for the Sb-substituted compositions compared to $La_{1.8}Sr_{0.2}CuO_4$. This suggests that the adsorption of methanol on the rare earth cuprates is more difficult compared to that on the platinum.

The apparent exchange current density values obtained for the rare earth cuprates and platinum are given in Table 5. It is seen from the values given in Table 5 that incorporation of Sb in the B-site improves the value of exchange current density suggesting increase in the electrocatalytic activity.

4. Conclusions

In the substituted rare earth cuprates, the active sites for methanol oxidation is deduced to be Cu(3 +) ions and the lattice oxide ions is considered as the active oxygen. The tolerance of the oxide electrode towards poisoning by the methanol oxidation intermediates depends on ease with which the lattice oxygen participates in the reaction with the methanol oxidation intermediates. The X-ray photoelectron spectroscopic data of C 1s region can be attributed to Sr carbonate species or adsorbed residues of methanol. The methanol oxidation onset potential depends on the type of transition metal ions in the B-site and the potential at which the redox reaction takes place. The methanol oxidation onset potential can be shifted to either cathodic or anodic side depending on the nature of the transition metal ion being partially substituted at the B-site. The high values of Tafel slopes obtained for rare earth cuprates compared to that of platinum in the methanol adsorption region suggest that the adsorption of methanol is probably the rate-determining step on these oxides.

References

[1] S.R. Parsons, T. Vandernoot, J. Electroanal. Chem. 257 (1988) 1.
[2] S. Wasmus, A. Kuver, J. Electroanal. Chem. 461 (1999) 14.
[3] T. Ohmore, K. Nodasaka, M. Enyo, J. Electroanal. Chem. 281 (1990) 331.
[4] J.B. Goodenough, R. Manoharan, M. Paranthaman, J. Am. Chem. Soc. 112 (1990) 1076.
[5] D.B. Meadowcroft, Nature 226 (1970) 30.
[6] J.O'M. Bockris, Z.S. Minevski, Electrochim. Acta 39 (1994) 147.
[7] T. Kudo, H. Obayashi, M. Yashida, J. Electrochem. Soc. 124 (1977) 321.
[8] J.O'M. Bockris, T. Otagawa, J. Electrochem. Soc. 131 (1984) 290.
[9] J.H. White, A.F. Sammells, J. Electrochem. Soc. 140 (1993) 2167.
[10] K. Hideki, T. Hashimoto, H. Tagawa, J. Mizusaki, Solid State Ionics 99 (1997) 193.
[11] T. Hyodo, M. Hayashi, N. Miura, N. Yamazoe, J. Electrochem. Soc. 143 (1996) L266.
[12] J. Mizusaki, Solid State Ionics 52 (1992) 79.
[13] J.B. Goodenough, Mater. Res. Bull. 8 (1973) 423.
[14] K. Hideki, T. Hashimoto, H. Tagawa, J. Mizusaki, Solid State Ionics 199 (1997) 193.
[15] S. Rajadurai, J.J. Carberry, B. Li, B. Alcock, J. Catal. 131 (1991) 582.
[16] V. Raghuveer, B. Viswanathan, Bull. Electrochem. 16 (4) (2000) 175.
[17] E. Rios, J.-L. Gautier, G. Poillerat, P. Chartier, Electrochim. Acta 44 (1998) 1491.
[18] K. Kishio, J.-I. Shimoyama, T. Hasegawa, K. Kitazawa, K. Fueki, Jpn. J. Appl. Phys. 26 (1987) L1228.
[19] M. Pourbaix, Atlas of Electrochemical Equilibria in Aqueous Solutions, National Association of Corrosion Engineers, Houston, TX, USA, 1976, 384.
[20] K.L.K. Yeung, A.C.C. Tseung, J. Electrochem. Soc. 125 (1978) 878.
[21] M. Fleischmann, K. Korinek, D. Pletcher, J. Electroanal. Chem. 31 (1971) 39.
[22] A.A. El-Shafei, J. Electroanal. Chem. 447 (1998) 81.

[23] A.A. El-Shafei, J. Electroanal. Chem. 471 (1999) 89.
[24] A.I. Vogel, A Text-Book of Quantitative Inorganic Analysis, 3rd edn., Longmans, Green and Co. Ltd., London, 1961, 249.
[25] L.G. Tejuca, J.L.G. Fierro, Adv. Catal. 36 (1989) 237.
[26] M. Yamazoe, Y. Teraoka, T. Seiyama, Chem. Lett. (1981) 1767.
[27] T. Nakamura, M. Misono, Y. Yoneda, J. Catal. 83 (1983) 151.
[28] S. Ebbinghaus, A. Reller, Solid State Ionics 101 (1997) 1369.
[29] R.G. Edgell, J.B. Goodenough, A. Hamnett, C.C. Naish, J. Chem. Soc., Faraday Trans. 1 79 (1983) 893.